FINITE ELEMENT ANALYSIS OF SHELL STRUCTURES

António Rui Fernandes Solheiro

Instituto Superior Técnico, Lisbon, Portugal

Summary

The aim of the work here reported is to perform structural analysis on shell structures using the Finite Element Method. The computational software used in this study is ADINA (Automatic Dynamic Incremental Nonlinear Analysis) [1].

A major case study is analysed in this work: the dome of the roman Pantheon. The roman Pantheon, a remarkable building more than 1800 years old, is the oldest concrete shell known and still the largest non-reinforced concrete (roman concrete) dome ever built. In this work, the influence on the elastic stress distribution on the dome of the stiffness of the support wall, the thickenings of its base and the use of different types of concrete are analyzed. The results are compared with similar nature studies carried out by Mark and Hutchinson [2] and by Morer and Goñi [3].

Following the study of the Pantheon, the study of shells is deepened. Considering the same geometrical conditions of the roman dome – the 43,3-meter circular span and the 9-meter oculus – the effect of varying cross-sectional dimensions and elevation is studied on a spherical shell.

Keywords: shell structures; Finite Element Analysis; roman Pantheon; spherical shells; dome;

1. Introduction

The purpose of this work was that of performing finite element analysis on shell structures.

Shell structures are laminar (meaning that one dimension is much smaller than the others) non-planar structures . It is due to their curvature that shells can balance applied loads primarily through in-plane forces, the membrane forces. This load-carrying behaviour makes of shells very efficient structures able to cover very large spans with a minimum amount of material, standing out from other structural solutions.

Being possible to achieve very slender solutions with high resistance and stiffness, it's frequent that, for thin shells subject to compressive forces, the critical stresses, associated with the instability of the shell, are the ones that limit the load-carrying capacity of the structure. In shell design, it is not uncommon also that construction requirements – as minimum spacing between rebars and covers – are the ones conditioning the minimum thickness that may be adopted for the structure.

Due to its complexity, the analysis of shell structures is particularly benefited by the use of appropriate finite element programs.

In this paper, we start the study of spherical shells by studying the dome of the Roman Pantheon. This hemispherical shell spanning a very large span is a remarkable example, for more than 1800 years now, of the best roman engineering and a legacy to mankind. The success of this robust shell, entirely executed on non-reinforced concrete, has, throughout the years, been linked to the thickenings of its base and the use of lightweight concretes in its upper regions. In this work, we perform a study similar to those of Mark and Hutchinson [2] and Morer and Goñi [3] and analyse the influence, on the elastic stress distribution on the shell, of the stiffness of the support wall, the thickenings of its base and the use of light concretes. The results obtained are then compared to both studies mentioned.

Following the study of the Pantheon's dome, with the purpose of deepening the knowledge of shells and of finite element modelling, starting from the same geometrical conditions that characterize the Roman dome – the circular 43,3-meter span and the oculus with a 4,5-meter radius at the apex – different solutions of spherical shells are formulated – by varying cross-sectional dimensions and elevation – and their behaviour with regards to buckling strength, stress distributions and maximum deflections is analysed. Finally, the buckling behaviour of an hemispherical shell considering the introduction of large displacements (geometrically non-linear) and geometrical imperfections is analysed.

2. Shell structures

A shell may be defined as a laminar structure that has curvature.

2.1. Load carrying behaviour of shells

It is due to their curvature that shells can carry applied loads primarily through in-plane stresses, the membrane stresses. These stresses are uniform on the thickness of the shell and the corresponding stress state is called membrane stress state. Bending moments and shear forces appear on shells (due to discontinuities in loading, geometry, or due to boundary conditions, for example) eventually only confined to very small regions, ensuring that most of the shell works in a membrane state of stress. It is important to notice that the presence of significant flexural stresses has no advantages on shell structures which, considering their small thickness, have very small resistance to such stress states. However, such stress states are generally confined to a very small region near the disturbance, region which gets smaller as the radius and the thickness of the shell decrease.

This behaviour of shells makes it possible to design very slender solutions in which the flexural problems are solved locally through special solutions.

Accordingly, the structural efficiency of shell structures is closely related to both its thickness and curvature.

2.2. Structural collapse of shells

A shell structure may collapse by instability, material failure or a combination of both.

2.2.1. Material failure

This collapse mode is related with the deterioration of the material properties of the shell and is more common in shells subjected to traction forces or compressed elements of low slenderness.

2.2.2. Buckling

When subjected to loads shells develop membrane forces and, if one of these forces is compressive, it is likely that instability of the shell occurs even before material failure, particularly for slender shells.

- **Post-buckling behaviour of shells**

When one of the membrane forces is of traction, it tends to bring the shell back to its initial configuration, allowing the shell to carry loads larger than the critical load in post-buckling regime (case 1). However, if both (principal) membrane forces are compressive they tend to increase the deformation of the shell after buckling occurs and so the shell can only carry loads smaller than the critical load in post-buckling (case 2). These two behaviours – very important to distinguish for shell design – are presented in Figure 2.1.

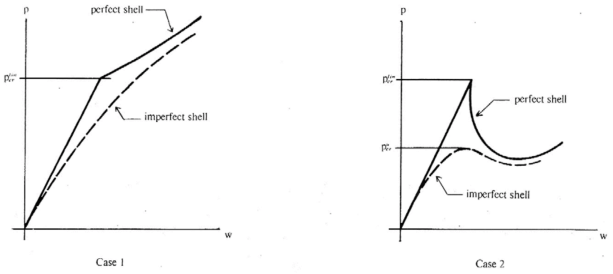

Figure 2.1 - Post-buckling behavior of shells - case 1 and case 2 [4].

- **Knockdown factor (C)**

There is a multitude of parameters that influence the real buckling strength of shells (as geometrical and material nonlinearities and geometrical imperfections) that may reduce its value in comparison to the theoretical critical load. Accordingly, it is current in shell design to use a reduction factor that accounts for all these parameters [4], this reduction factor (C) if multiplied by the theoretical critical load will give its real buckling load:

$$p_{cr}^{real} = C \cdot p_{cr}^{theoretical}. \quad (1)$$

2.3. Elastic Theory of Shells

The Elastic Theory of Shells establishes the basic quantities used to describe the behaviour of shells – displacements, strains and stresses – as the equations that allow their correlation – compatibility, equilibrium and elasticity. Elastic Theories of Shells, may be divided in two groups: first order and higher order theories. In first order theories, the thickness of the shell is assumed small in comparison not only to its other dimensions but also to the minimum radius of curvature of the undeformed midsurface. The effect of normal stresses to the midsurface is neglected and it is assumed that the shell deforms in a way that fibers that are normal to the midsurface at its undeformed configuration remain normal and of the same length after deformation (Kirchhoff hypothesis). Higher order theories are refined theories with presumably more precise results that revise one or many of the assumptions of first order theories. In Reissner's theory, Kirchhoff's hypothesis is modified so that the fibers that are initially normal to the midsurface, do not necessarily remain normal after deformation. In higher order theories for moderately thick shells, the thickness to radius of curvature ratio is not considered small, and so is not neglected. For the study of the Elastic Theory of Shells, the reference book "Theory and Analysis of Elastic Plates and Shells" by J.N. Reddy [5] is recommended.

3. The Finite Element Method

The Finite Element Method (FEM) is a method of numerical analysis to obtain approximate solutions to problems defined by systems of partial differential equations and respective boundary conditions. This method can be applied to obtain solutions for the compatibility, constitutive and equilibrium equations resulting from the application of the different theories of elasticity. The increase in computational power in the last years has stimulated the use of Finite Element Analysis (FEA) for structural design. Complex calculations which could not be performed before, can now be solved with precision and time efficiency using one of many FEM computer codes available. The analysis of shell structures is particularly favored by the use of FEM software, making it possible to analyze problems with complex geometries, boundary and loading conditions. Despite the obvious advantages of using FEM for structural analysis and design, it is important to be aware that, if improper modelling options are taken or errors occur in the input parameters, the results may be inaccurate. It is very important then, that an engineer has good knowledge of both the FEM and the theories of elasticity that govern the problems being analysed, in order to be confident in the results obtained by FEA. For the study of the Finite Element Method the reference book "Finite Element Procedures" by K.J. Bathe [6] is recommended.

4. Finite Element Analysis of Shells

In this section, the Finite Element Analysis of shells is performed.

4.1. The dome of the roman Pantheon

The roman Pantheon is one of the most important monumental buildings of ancient Rome, it was built during AD II as a temple to all divinities of Pagan Rome. Its architecture, the massive dome covering the main room, as well as the roman concrete that constitutes the main structure of the building make the Pantheon a landmark in engineering history and a legacy to mankind.

4.1.1. Geometry, structure and materials of the Pantheon

The building of the Pantheon (Figure 4.1) may be divided in three main and clearly defined parts: the porch, the intermediate block and the rotunda covered by the hemispherical dome. In this paper, we will focus on the assembly dome-rotunda, considering that the porch and the immediate block are not supporting the dome.

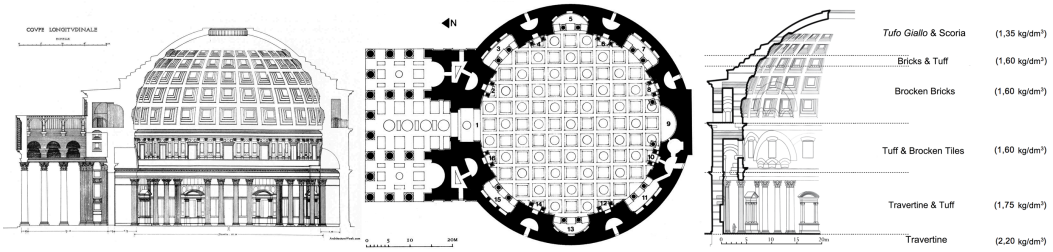

(a) (b) (c)

Figure 4.1 – Longitudinal profile of the Pantheon [7], plan of the Pantheon [8] and aggregate types and corresponding unit weights, according to Terenzio [9] and adapted from Lancaster [10].

The rotunda is a 6-meter thick concrete cylindrical wall covered with about 60 cm of brick, containing cavities, chambers and large exits arranged on three levels [10]. The diameter of the rotunda, 43,3 meters in the interior, corresponds exactly to the height of the hemispherical dome. The base of the dome, externally, is embed by the upper part of the cylindrical drum, which forms a circular terrace, slightly inclined towards the outside. The exposed portion of the dome features a series of seven stepped rings (Figure 4.1). The first ring has a thickness of 2,25 meters and the following six have an inward slope of 1:10 and the last ring starts at 47° from the axis. The intrados, or the inner surface of the dome, is divided, up to about two-thirds of its height, into 5 levels of coffers distributed radially around a central oculus with a diameter of 9 meters. Disregarding the voids due to the coffering, the dome has an approximately constant thickness of 1,5 meters added at its base to the upper part of the cylindrical wall and the seven stepped rings.

The material composition of the Pantheon was documented by several authors such as Terenzio [9], MacDonald [8], or, more recently Lancaster [10]. According to MacDonald, the intermediate block, the rotunda and the dome are made almost entirely in concrete, the bricks observable in the cylinder being a mere covering on this structure, although there are here and there some structural elements in stone.

The mortar developed by the Romans for their concrete is obtained by combining, in carefully controlled proportions, Pozzolan (fine volcanic ash), lime and water. The romans were very conscious of the composition of their materials and the Pantheon is composed of concrete with varying aggregates (*caementa*), from the heavier and more resistant travertine pieces at the foundation level to the lightweight aggregates of yellow tuff and Vesuvian scoria at the top of the dome (Figure 4.1 (c)).

There is no material model for each of the different formulations of concrete applied in the Pantheon, as there are no testable samples of such concrete. In this work, the mechanical properties selected to characterize the mechanical behaviour of Roman concrete (Table 4.1) are based on studies of Roman concretes by different authors. Both the elastic modulus (E_c) and compressive strength (f_c) of the material are obtained by the results of Ferretti [11] from samples of Adrian Villa, contemporary of the Pantheon and located in the same region. The value of the maximum tensile strength (f_t) of the concrete is taken from the study of Jackson *et al.* [12]. The Poisson coefficient (υ) is assumed, by hypothesis, equal to 0,2.

Table 4.1 - Mechanical properties selected to characterize the concrete of the Pantheon.

E_c [GPa]	ν	f_c [MPa]	f_t [MPa]
2,9	0,2	3,6	1,1

4.1.2. Some relevant studies of structural analysis of the Roman Pantheon

The prominence of the Pantheon among Roman monumental buildings, has aroused the curiosity of various authors, raising different hypotheses about the performance of various aspects of its structure and constituent materials, so there are several studies of great interest of analysis of this edifice.

Mark and Hutchinson [2] and Morer and Goñil. [3] perform studies of application of the Finite Element Method to the structural analysis of the Roman Pantheon. In both studies the rotunda-dome assembly is modelled as an axisymmetric problem and the elastic stress distributions are analysed under the self-weight of the structure. The structure is modelled with a geometry of growing complexity including or not the varying weight of the concretes, in order to examine the influence of various components of the structure.

The analysis presented here are alike those of studies [2] and [3] and the results are compared.

4.1.3. Analysis of the dome-rotunda assembly with finite elements

In this section, structural analysis of the assembly dome-rotunda is performed with finite elements.

4.1.3.1. Modelling details

In the structural modelling process, simplistic assumptions are adopted for geometry, material properties, and boundary conditions. Both studies mentioned [2] and [3] have similar assumptions and such assumptions are also followed here for their reasonableness and so that results obtained may be directly comparable.

Geometry: only the rotunda-dome assembly is modelled. The model is axisymmetric, assumes the rotunda to be solid, integrally in concrete, and of constant thickness of 5,5 meters. The thickness of the dome is assumed constant with 1,5m at the top added by the thickenings at the lower regions.

Support conditions: it is considered that the rotunda wall is fixed at the ground level.

Material properties: the material is assumed linear elastic and isotropic. The mechanical properties E_c and ν adopted for the material model are summarized in Table 4.1. The values of the maximum stresses f_c and f_t are taken as references to analyse de values of the stresses obtained. The unit weights adopted for the different concrete formulations are in accordance with Figure 4.1 (c).

4.1.4. Models 1 to 7

To examine the influence of different parts of the structure and of the varying weight of concrete, a number of different models are developed and tested (Figure 4.2).

Models (M) 1, 2 and 3, formed by shell elements MITC16 (Mixed Interpolation Tensorial Components) [13], are composed only by the dome and varying the support conditions, being simply supported, pinned and fixed, respectively.

Models 4 to 6 are formed by 2D axisymmetric elements and model the assembly rotunda-dome. Model 4 is formed by the hemispherical dome of uniform thickness embed directly over the rotunda. Model 5 adds to Model 4 the upper part of the rotunda, covering the base of the dome. Model 6 adds the stepped rings to Model 5. All models described (1 to 6) are composed by the lighter concrete (1,35 kg/cm^3), described in Figure 4.1.

Model 7 has the same geometry of Model 6 but has concrete of varying weight, according to Figure 4.1.

A Model 6P is developed to clarify the effect of adopting light concretes in the upper regions (comparing to Model 7) so, this model, is equal to Model 6 but uses the heaviest concrete (2,20 kg/cm^3).

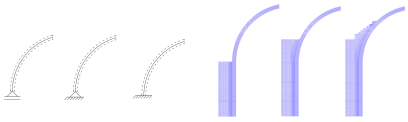

Figure 4.2 – Geometry of finite element models 1 to 7.

4.1.5. Analysis results

Figure 4.3 shows the stress distributions on the outer surface of the dome for Models 1 to 3 and Figure 4.4 shows the stresses on the cross section of Models 4, 5, 6 and 7, respectively.

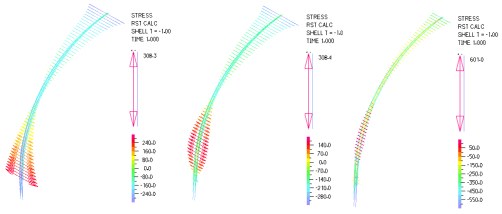

Figure 4.3 – Stress distributions on the outer surface of the shell for Models 1, 2 and 3, respectively [kN/m^2].

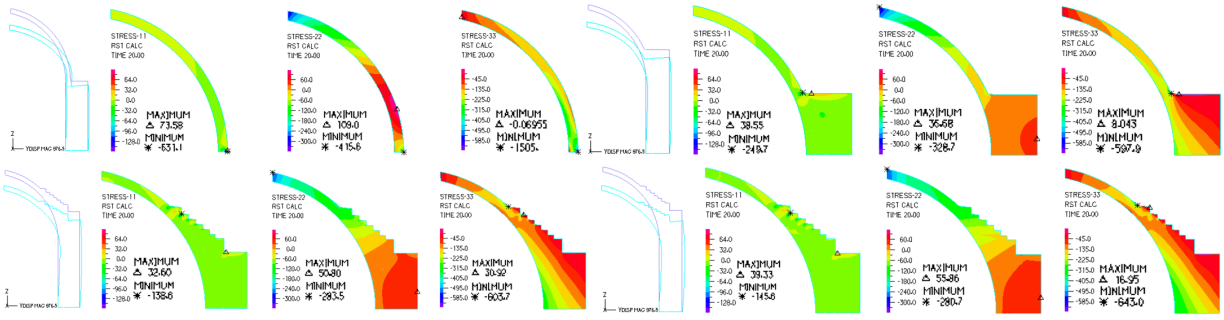

Figure 4.4 - Hoop and meridional stresses for models 4, 5, 6 and 7 ($22 \equiv \theta\theta$ and $33 \equiv \varphi\varphi$) [kN/m^2].

Table 4.2 shows the values of the maximum and minimum hoop and meridional stresses on the dome for the models 1 to7.

Table 4.2 – Maximum and minimum hoop stresses and meridional stresses for models 1 to 7.

Model	Author	Hoop stresses $(\sigma_{\theta\theta})[\mathbf{kN/m^2}]$		Meridional stresses $(\sigma_{\varphi\varphi})[\mathbf{kN/m^2}]$	
		Maximum value	Minimum value	Maximum value	Minimum value
1	ADINA	295,00	-326,20	-0,54	-300,60
	Mark & Hutchinson	323,619	*	*	*
	Morer & Goñi	215,746	*	*	-284,393
2	ADINA	155,00	-326,20	-0,54	-456,60
3	ADINA	105,20	-327,80	77,03	-650,10
4	ADINA	109,00	-415,60	-0,07	-1505,00
	Mark & Hutchinson	98,07	*	*	*
	Morer & Goñi	118,66	-274,59	*	*
5	ADINA	36,68	-328,70	8,04	-597,90
	Mark & Hutchinson	49,03	*	*	*
	Morer & Goñi	58,84	-274,59	*	*
6	ADINA	50,80	-283,50	30,92	-603,70
6P	ADINA	82,76	-461,86	50,37	-983,60
	Mark & Hutchinson	107,87	*	*	*
	Morer & Goñi	58,84	-416,78	*	*
7	ADINA	55,86	-280,70	16,95	-643,00
	Mark & Hutchinson	63,74	*	*	*
	Morer & Goñi	24,52	-264,78	*	-264,78

*non-given values.

4.1.6. Conclusions

- The results obtained by the ADINA models are in good accordance with references [2] and [3].
- Comparing the values from models 1,2,3 and 4, one can understand that the dome is nearly fixed on the rotunda.
- Comparing models 4 and 5 it is noticeable that the rise of the rotunda largely decreases the values of the maximum elastic hoop stresses in the dome.
- Comparing models 5 and 6, it's noticeable that the stepped rings increase the maximum hoop stresses in the dome.
- Comparing models 6P and 7, it's perceptible a large decrease in maximum hoop stresses.
- The values of the observed stresses are much lower than the elastic limits obtained from experimental data of roman concretes.

4.2. Variations on the Pantheon: Parametric studies of spherical shells

In this section, different solutions for the same geometrical conditions of the roman Pantheon's dome: the 43,3-meter span, the spherical geometry and the circular oculus at the apex, considering current materials and regulations, are formulated and analysed.

4.2.1. Previous considerations

Previously to the development of the following studies, it is necessary to limit their scope - some assumptions regarding support conditions, materials and actions are taken.

- **Support conditions**
  The shell is assumed pinned in its entire perimeter.
- **Material**
  The material is assumed to be a C35/38 lightweight concrete (Table 4.3) and in all analysis performed the material is considered isotropic and linear elastic.

Table 4.3 – Properties of lightweight concrete C35/38, according to the manufacturer [14].

γ [kN/m^3]	E_c [GPa]	ν	f_{ck} [MPa]	f_{cd} [MPa]	f_{ctm} [MPa]
20	22,8	0,2	35	23,3	2,85

- **Loads and load combinations**
  The following studies consider as dead load (d.l.) the self-weight of the structure and the wind and the snow as variable loads (v.l.), defined according to EN1991-1-4 (2010) and EN1991-1-3 (2009), respectively, considering the location and altitude of the Roman Pantheon, according to Italian National Annex.
  The wind load considers the division of the dome in three regions (Figure 4.5, on the left), the values of the wind action on each region are presented on Table 4.4 for the domes studied in this paper.

Table 4.4 – Values of external wind pressure (w_e) on regions A, B and C of the domes.

Rise of the dome [m]	5			10			21,65		
Zona	A	B	C	A	B	C	A	B	C
$w_e\ [^{kN}/_{m^2}]$	-1,85	-1,26	-0,62	0,13	-1,51	-0,64	1,35	-2,02	-0,67

Snow load model considers two situations, namely undistributed (u.s.l.) and redistributed (r.s.l.). For undistributed snow the load value is uniform over the surface and for redistributed snow the load pattern adopted is presented on Figure 4.5, as recommended by Matten [15] for spherical shells.

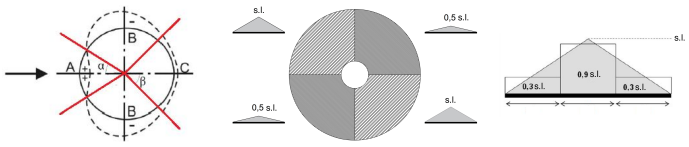

Figure 4.5 – Wind regions on the dome, load shape for redistributed snow on the shell surface and loading simplification adopted for r.s.l. [15].

According to EN1991-1-3 (2010), snow load is only applied where the inclination of the shell is smaller than 60º. The values for s.l. for the different rises of the shells studied in this paper are presented in Table 4.5.

Table 4.5 – Values of the snow load on the domes with different elevations.

Rise of the dome [m]	5	10	21,65
Undistributed s.l. [kN/m^2]	0,48	0,48	0,48
Redistributed s.l. [kN/m^2]	0,41	1,51	3,12

Finally, two load combinations are considered in this study, for Ultimate Limit States (ULS) and Service Limit States (SLS), respectively:

$$1{,}35 \cdot (d.l.) + 1{,}5 \cdot (v.l.) \quad (2)$$

$$1{,}0 \cdot (d.l.) + 0{,}2 \cdot (v.l.). \quad (3)$$

4.2.2. Formulation of possible cross-sections

Two types of cross-sections for the hemispherical sphere are formulated: uniform and ribbed.

4.2.2.1. Thickness of the dome

As it is of interest, in this work, to have a solution with minimum amount of material, we consider the guidelines on the minimum thickness of shells given by the reference document for shell design by IASS [4] and by the norm EN1992-1-1 (2010).

The document by IASS [4] indicates that 50mm is the minimum thickness that allows for good concreting and placement of reinforcement in a shell. However, the norm EN1992-1-1 (2010) is more restrictive: considering an exposure class XC4 and a structural class S6 (for a life-span of 100 years), one gets a minimum cover over the rebars of 40mm; considering two rebar meshes of 8mm diameter, a distance between different meshes of 20mm, the minimum thickness of the shell becomes 132mm. It is decided to study the following uniform thicknesses: 50, 100, 132 and 200mm.

4.2.2.2. Ribbed cross-sections

To define the ribbed solutions, the shell is considered divided in 24 ribs (15º between ribs) along the meridians and 10 ribs along the parallels (7,8º between ribs). The ribbed solution is thought for a shell divided into small panels, that may be pre-casted and just have the need to be placed in site and connected through proper connectors applied on the ribs.

Two ribbed cross-sections are defined (Figure 4.6): the first ribbed cross-section (ribbed 1) is obtained through material redistribution and has approximately the same amount of material that the solution of 200mm (uniform thickness); the second ribbed cross-section (ribbed 2), has the same dimensions for the ribs as those of “ribbed 1”, but reduces the thickness of the inner shell.

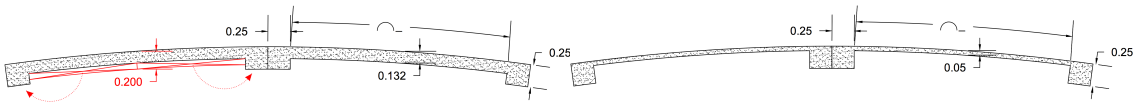

Figure 4.6 – Scheme of material redistribution on shell cross-section and dimensions of sections: ribbed 1 and 2.

4.2.3. Rise of the dome

Two different elevations are studied (apart from the hemispherical solution), considering the 43,3-meter span, the uniform thickness of 132mm and the oculus at the top of 4,5-meter radius. In concrete shells, it is of interest to have only compressions, so, imposing the condition of having compressive membrane hoop forces ($N_{\theta\theta}(\phi) < 0$) on the entire shell domain, through equation (4), given by the Membrane Theory of Shells [16] for a spherical shell under dead load with ϕ aperture and oculus with an opening angle ϕ_0:

$$N_{\theta\theta}(\phi) = -\frac{1}{\sin^2\phi}\left[q \cdot R(\cos\phi \sin^2\phi - \cos\phi_0 + \cos\phi)\right], \quad (4)$$

the following elevations are chosen: 10 and 5 meters (with span-to-rise ratios of 4,33 and 8,66).

4.2.4. Validation criteria

The different solutions formulated are analysed for buckling strength in ULS, stress distributions in ULS and maximum deflections in SLS, for the load combinations defined on section 4.2.1.

4.2.4.1. Buckling in Ultimate Limit States

Adopting a knockdown factor (C) of 1/6, a solution is considered safe with respect to buckling in ULS if the critical load coefficient (λ_{cr}) is larger than 6.

4.2.4.2. Stress distributions in Ultimate Limit States

In this work it is not intended to dimension (design) the reinforcement on the section of the solutions but to compare their behaviour for different dimensions. An order of magnitude for the stress distributions in ULS may be obtained by comparing its values to the material resistance. The values of the maximum membrane forces may be compared with the resistance in compression of the concrete section and in traction of the reinforcement steel adopted. The maximum resisting compressive (N_{rd}^{-}) and tractive (N_{rd}^{+}) membrane forces of the section are given by:

$$N_{rd}^{-} = f_{cd} \cdot h \quad \text{and} \quad N_{rd}^{+} = f_{yd} \cdot A_s \tag{5}$$

, where f_{yd} is the design yield stress of the steel (435MPa for A500NR) and A_s is the reinforcement area/m.

4.2.4.3. Deflection in Service Limit States

To verify safety for deflection in SLS, the value for long term maximum deflection (δ_∞), obtained from elastic deflection (δ_e) considering concrete creep coefficient (φ), is compared with the span (L):

$$\delta_\infty = \delta_e \cdot \left(1 + \varphi(\infty, t_0)\right) \approx \delta_e \cdot 3{,}5 < L/500. \tag{6}$$

According to expression (5), if

$$\delta_e < \frac{L}{500 \cdot 3{,}5} = \frac{43300}{500 \cdot 3{,}5} = 24{,}74mm, \tag{7}$$

the solution verifies safety for Deflection in Service Limit States.

4.2.5. Finite Element Analysis of spherical shells

The various FEA analysis performed on the selected cases are presented in this section.

4.2.5.1. Linearized buckling analysis for Ultimate Limit States

The various geometries defined in previous sections are now compared for their buckling behaviour in ULS. In Figure 4.7, the first buckling mode for the hemispherical simple shells, for shells ribbed 1 and ribbed 2, and for the shells with rise-to-span ratio of 4,33 and 8,66, respectively are shown.

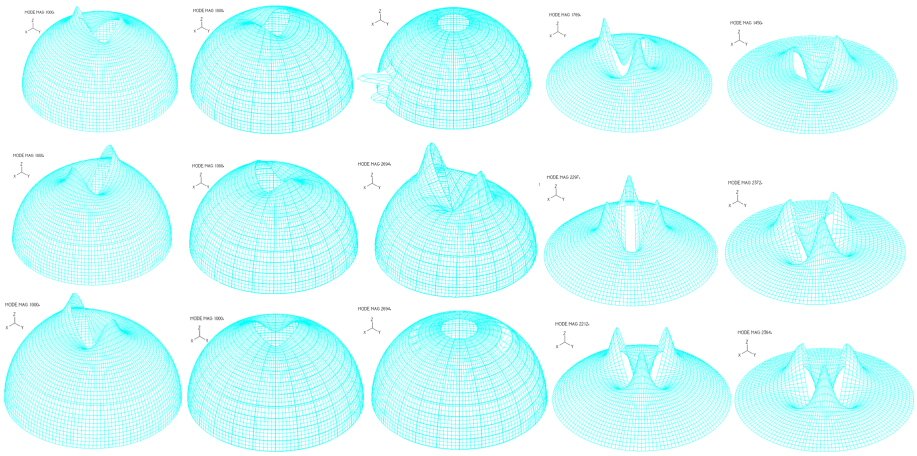

Figure 4.7 – First buckling mode in ULS for the various solutions for wind (top), u.s.l. (middle) and r.s.l. (bottom).

The corresponding critical load coefficients (λ_{cr}) are shown in Table 4.6.

Table 4.6 - Critical load coefficients (λ_{cr}) corresponding to the first buckling mode for ULS.

Span-to-rise ratio	**2**						**4,33**	**8,66**
Section	**50 mm**	**100 mm**	**132 mm**	**200 mm**	**ribbed 1**	**ribbed 2**	**132mm**	**132mm**
λ_{cr} (wind)	5,89	26,07	36,62	73,43	104,34	80,94	62,31	32,77
λ_{cr} (u.s.l.)	7,28	28,20	41,46	77,59	99,11	100,52	35,09	16,48
λ_{cr} (r.s.l.)	6,00	24,38	37,13	72,09	94,35	77,45	37,07	18,56

4.2.5.2. Linear static analysis

The distributions of the membrane forces ($N_{\varphi\varphi}$, $N_{\theta\theta}$, $N_{\theta\varphi}$) are displayed in Figure 4.8 and the distributions of bending moments ($M_{\varphi\varphi}$, $M_{\theta\theta}$, $M_{\theta\varphi}$) and shear forces (Q_{φ}, Q_{θ}) are shown on Figure 4.9, for the different cases.

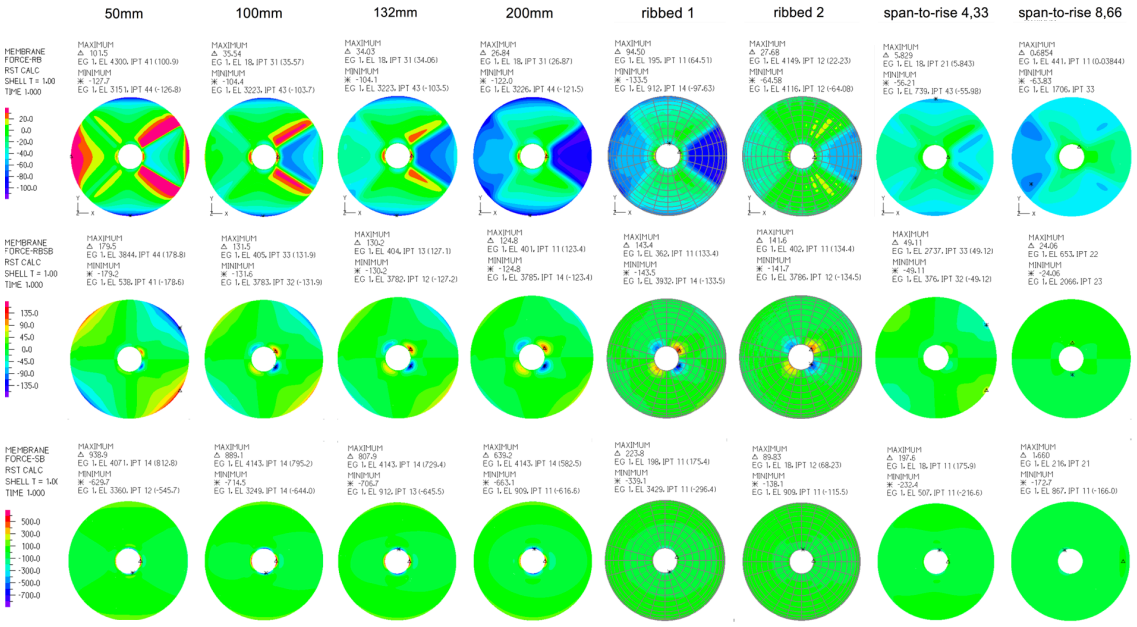

Figure 4.8 - Distributions of membrane forces ($N_{RB} \equiv N_{\varphi\varphi}$, $N_{SB} \equiv N_{\theta\theta}$, $N_{RBSB} \equiv N_{\theta\varphi}$) [kN/m] for ULS (wind as v.l.).

Figure 4.9 - Distributions of $M_{RB} \equiv M_{\varphi\varphi}$, $M_{SB} \equiv M_{\theta\theta}$, $M_{RBSB} \equiv M_{\theta\varphi}$ [kNm/m] and $Q_{RB} \equiv Q_{\varphi}$, $Q_{SB} \equiv Q_{\theta}$ [kN] for ULS (wind as v.l.).

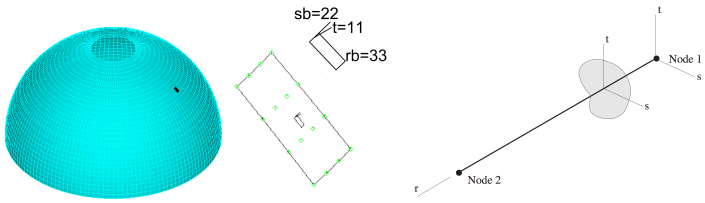

Figure 4.10 - Local referential of *MITC16* shell elements and of *beam elements* (Adapted from *ADINA R&D* [13]).

The extreme values of the axial forces (N), bending moments (M_s e M_t) and shear forces (Q_s e Q_t) on the ribs for solutions: ribbed 1 and ribbed 2 are presented on Table 4.7.

Table 4.7 - Maximum and minimum values of N, M_t, M_s, Q_t and Q_s on the ribs in ELU for wind as v.l. (connected ribs with resulting section of 0,50x0,25 m^2).

Section	N[kN]	M_t[kNm]	M_s[kNm]	Q_t[kN]	Q_s[kN]
ribbed 1	170,01 -280,80	42,67 -51,28	∓4,07	∓8,73	∓30,33
ribbed 2	221,02 -332,34	53,00 -62,88	∓10,64	∓18,65	∓35,17

The values of the maximum vertical deflections for SLS on the solutions are shown on Table 4.8.

Table 4.8 – Maximum vertical (gravity direction) deflections for SLS for the formulated solutions.

Span-to-rise ratio	**2**						**4,33**	**8,66**
Section	**50 mm**	**100 mm**	**132 mm**	**200 mm**	**ribbed 1**	**ribbed 2**	**132mm**	**132mm**
δ_e **(wind)** $[mm]$	21,94	5,85	5,85	1,66	1,43	1,79	1,32	1,22
δ_e **(u.s.l.)** $[mm]$	1,00	0,72	0,71	0,70	0,63	0,75	0,53	1,15
δ_e **(r.s.l.)** $[mm]$	3,84	1,56	1,16	0,87	1,04	1,31	0,69	0,84

The stress values are always higher (in absolute value) for the load combination that has the wind as variable load and so, only these results are presented in this document.

4.2.5.3. Simulation of non-linear behaviour of hemispherical shell

In this section, the geometrically non-linear behaviour of the hemispherical solution with h equal to 132mm is analysed. The following analyses are intended to evaluate the effects of the large deflections (geometrically non-linear behaviour) and the presence of geometry imperfections on the buckling resistance of the shell. In the present section, only r.s.l. is considered but two load situations are analysed: the simultaneous increment of d.l. and r.s.l. and the increment of r.s.l. only, not considering d.l.. The two load situations described are intended to analyse if the simultaneous increase of d.l. and r.s.l. is a safe option for buckling analysis, as adopted in linearized buckling analysis on section 4.2.5.1. The geometrical imperfections considered correspond to the buckling pattern obtained for each load situation (Figure 4.7 bottom left for d.l. plus r.s.l.).

To define the load pattern, the value of the maximum initial imperfection is imposed at a selected node. According to IASS [4], the maximum value of the imperfection (w_0) may be proportional to the thickness ($0 < w_0 < h$), in this work, we adopt w_0 to be 66mm ($h/2$). The node of control selected for the analysis is the node that displayed the largest displacement in linear static analysis, located on the border of the oculus.

The results of the non-linear analysis performed by the arch-length-method (see [17]) are shown in Figure 4.11.

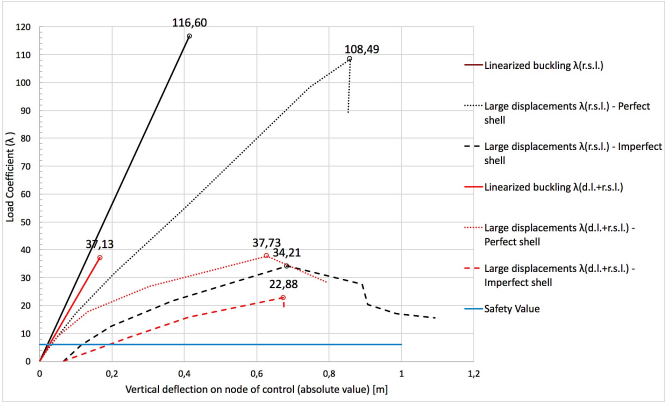

Figure 4.11 – Load coefficient *vs* vertical displacement on node of control – hemispherical solution (h =132mm).

The results of such analysis allow to evaluate the safety of adopting a buckling reduction factor (C) of 1/6.

4.2.6. Conclusions

- All solutions verify buckling safety for ULS except for the solution that has uniform thickness of 50mm.
- Loads are balanced mainly by membrane forces being that bending moments and shear forces are nearly zero throughout the domain of the different cases. Significant bending moments and shear forces appear near the oculus, particularly for the load combination that has the wind as variable action. This fact may justify the option for reinforcing the border of the oculus with a reinforcing ring.
- Solutions that have thicknesses smaller than 132mm, although having adequate compressive forces, do not allow for the placement of reinforcement able to resist the traction stresses on the shell respecting the minimum covers and spacing according to EN 1992-1-1 (2010). The solution with 100mm thickness allows only for the placement of one layer of rebars and may have problems in resisting even the small bending moments that appear in the domain of the shell.
- All solutions have acceptable maximum deflections for the load combinations considered.
- As the thickness decreases: the values of the main membrane forces, the bending moments and shear forces increase; the value of the maximum deflection increases; buckling resistance diminishes.
- The formulation of a ribbed cross-section, with nearly the same amount of material (ribbed 1) lead to: stiffer solutions with 31% higher buckling strength; a reduction of about 14% of the maximum deflection; a very significant reduction on the values of the shear forces and the bending moments observable at the oculus region of the shell for the simple solutions (the ribs absorb almost all these efforts, remaining only residual stresses and small shear forces near the edges of the higher panels, close to the ribs); an increase of the values of the maximum membrane forces $N_{\varphi\varphi}$ and $N_{\theta\varphi}$, although, the more limiting $N_{\theta\theta}$ forces, reduced to nearly 50% for the maximum compressions and to 35% for the maximum tractions.
- The reduction of the thickness of the panels between ribs originated problems of local instability for the first and third load combinations, compromising the buckling resistance of the solution.
- The maximum forces and bending moments on the ribs are reasonable and do not limit the solutions.
- As the rise of the dome is reduced: the area of the shell subject to membrane forces of traction diminishes and its peak tractions were hugely lowered, for the load combination that has the wind as variable load; both principal membrane forces are compressive in the whole domain, for the load combinations that have the snow as variable load, as consequence of the pre-dimensioning condition; the values of bending moments and shear forces that arise near the oculus closely disappear for the shallower solutions, remaining only significant Q_θ for the solution with 10-meter elevation, confined to a very small region on the border of the opening; the buckling resistance diminishes, although, for the 10-meter high solution the buckling resistance is nearly the same as that of the hemispherical solution but with a much smaller amount of material; the values of the maximum deflections diminished for shallower solutions for the wind as v.l. but increased for the solution with 5-meter elevation under snow load.
- The analysis of the results obtained from the non-linear analysis performed on the hemispherical shell with uniform thickness of 132mm allow for the following conclusions: the option to increment both loads (dead and snow load) as opposed to increasing only the snow load is a safe option; the introduction of the large displacements on the analysis of the perfect shell does not have a big influence on reducing the buckling resistance of the dome (comparing to the results obtained by linear analysis); the hemispherical shell open at the apex is very sensitive to geometrical imperfections, showing a decrease of 68% and 38% on the buckling resistance for the case where only v.l. is increased and both loads (d.l. and v.l.) are increased, respectively; the value of the buckling reduction factor (C) of 1/6 adopted is on the safe side, although the influence of physically non-linear effects was not accounted (usually the reduction due to material non-linearities is smaller than that due to geometrical non-linearity and geometrical imperfections); the hemispherical shell with the open apex shows a post-buckling behaviour typical of synclastic shells (case 2, Figure 2.1): after instability occurs the shell can only carry loads smaller than the critical one.

5. Closure and future developments

In this work the analysis of shell structures by the Finite Element Method was performed. The roman Pantheon was developed as case-study and the effect on stress distributions on the structure was analysed under self-weight for models of growing complexity. Following the study of the Pantheon, different solutions for the same geometrical conditions – the 43,3-meter circular span and the 4,5-meter oculus - were formulated and analysed. The effects of varying cross-section dimensions and elevation on buckling resistance, stress distribution and maximum deflection were studied for spherical shells with an opening at the top. The effect of geometrically non-linear behaviour and the presence of imperfections on the buckling resistance of an hemispherical shell were also studied.

In addition to the work carried out, the following future developments are suggested: analyse the behaviour of the Pantheon structure subject to other loads such as snow, wind and seismic actions; analyse the influence of the stepped rings on the stability of the Pantheon; consider the effect of the oculus on the modelling of wind action; calculate the linear critical loads keeping the self-weight constant and increasing only the variable load; dimension the reinforcements of the 132mm section and confirm the possibility of reinforcing the section with two meshes of ø8 rods; investigate the possibility of designing the shell with only one layer of rebars; study the non-linear behaviour of the remaining solutions and consider the other load combinations; introduce physical nonlinearities in geometrically non-linear models; compare the results obtained from the non-linear analyses with experimental results.

References

[1] I. ADINA R&D, *ADINA,* Watertown, Massachusetts: ADINA R&D, Inc., 2016.

[2] R. Mark and P. Hutchinson, "On the Structure of the Roman Pantheon," in *The Art Bullettin*, vol. 68, College Art Association, 1986, pp. 24-34.

[3] P. Morer and R. Goñi, "A benchmarking study of the analysis of non-reinforced structures applied to the structural behavior of domes," in *Structural Analysis of Historic Construction*, Londres, Taylor & Francis Group, 2008, pp. 705-713.

[4] The Working Group on Recommendations of The International Association for Shell and Spatial Structures, Recommendations for reinforced concrete shells and folded plates, Madrid: IASS, 1979.

[5] J. N. Reddy, Theory and Analysis of Elastic Plates and Shells, Segunda Edição ed., Boca Raton: CRC Press, 2006.

[6] K. J. Bathe, Finite Element Procedures, Nova Jersey: Prentice Hall, 1996.

[7] G. Gromort, "Architectureweek," Abril 2017. [Online]. Available: http://www.architectureweek.com/cgi-bin/awimage?dir=2005/0831&article=culture_1-2.html&image=12796_image_5.jpg.

[8] W. D. MacDonald, The Pantheon: Design, Meaning and Progeny, Segunda Edição ed., Cambridge: Harvard University Press, 1976.

[9] A. Terenzio, "La restauration du Panthéon de Rome," in *La conservation des monuments d'art & d'historie*, Paris, Institut de cooperation intellectuelle, 1934, pp. 280-285.

[10] L. C. Lancaster, "Materials and Construction of the Pantheon in Relation to the Developments in Vaulting in Antiquity," 2009, pp. 117-125.

[11] A. S. Ferretti, "Proposte per lo studio teorico-sperimentale della statica dei monumenti in opus caementicium.," in *Materiali e Strutture 7*, 1997.

[12] M. Jackson, B. Scheetz, D. M. Deocampo and F. Marra, "Assessment of material characteristics of ancient concretes, Grande Aula, Markets of Trajan, Rome," *Journal of Archaeological Science,* Novembro 2009.

[13] I. ADINA R & D, Theory and Modeling Guide Volume I: ADINA Solids & Structures, Massachusetts: ADINA R & D, Inc., 2012.

[14] Unibetão – Indústrias de Betão Preparado, S.A., [Online]. Available: www.unibetao.pt. [Accessed Abril 2017].

[15] R. N. Maten, "Ultra High Performance Concrete in Large Span Shell Structures," 2011.

[16] E. Ventsel and T. Krauthammer, Thin Plates and Shells - Theory, Analysis, and Applications, Pennsylvania: Marcel Dekker, Inc., 2001.

[17] N. Vasios, "Nonlinear Analysis of Structures The Arc Length Method: Formulation, Implementation and Applications," Harvard University Press, 2015.

[18] J. A. Teixeira de Freitas, Análise de Estruturas II: Elasticidade Plana e Tridimensional, Lisboa: IST Press, 2015.